Auger Recombination Processes and Threshold Conditions in Asymmetric-Multiple-Quantum-Well Heterostructure Lasers

I.A. SUKHOIVANOV
Guanajuato Univ.
Salamanca
MEXICO

O.V. MASHOSHINA
Kharkov National Univ. of Radio Electronics
61166, Lenin Ave., 14, Kharkov
UKRAINE

V.K. KONONENKO, D.V. USHAKOV
Stepanov Inst. of Physics NASB
Fr. Scorina Pr., 70, 220072 Minsk
BELARUS

Abstract: - Different possible processes of non-radiative Auger recombination which occur in the active region of quantum-well lasers are analyzed and the temperature dependence of the lasing threshold in the GaInAs-GaInAsP-InP bi-quantum-well heterolasers with different widths of the quantum wells (4 and 9 nm) is determined. Activated behavior of the Auger recombination is mentioned and respective effective parameters of the processes are calculated. For described asymmetric quantum-well heterostructure lasers, it is shown that the influence of the Auger recombination processes on the temperature behavior of the lasing threshold is not essential until the temperature of the active region is lower than 360 K and the cavity losses do not exceed 80 cm^{-1}.

Key-Words: - Auger recombination, asymmetric quantum-well laser, gain, threshold, temperature parameters

1 Introduction

Basic components of modern telecommunication systems are lasers operating at the wavelength 1.55 μm where the optical fiber losses are minimal. The laser diodes must be stable and have low values of the threshold current. At the operation temperature enhancement, the lasing threshold increases mainly because of Auger recombination (AR) processes accelerating [1]. While the long-wavelength lasers development it is important to get the weakening of such processes. A plausible way for solving this problem can be application of semiconductor lasers based on asymmetric quantum-well (QW) heterostructures [2]. These laser heterostructures can serve as broadband light sources for multi-channel fiber-optical network systems [3].

In the work, the temperature dependence of the lasing threshold in the GaInAs-GaInAsP-InP bi-QW heterolasers with different widths of the QWs (4 and 9 nm) has been determined. Including into consideration the processes of non-radiative AR allows to take into account the non-equilibrium processes which occur in the active region of the QW lasers more completely and accurately.

2 Theory

2.1 Lasing Threshold

In the general case, the threshold current in QW heterostructure lasers j_{th} is determined by the threshold quantity of the spontaneous radiative recombination rate R_{sp} in the active region, i. e.,

$$j_{th} = \frac{ed}{\eta'\eta_{sp}} R_{sp}, \qquad (1)$$

where d is the QW width, η' is the injection efficiency, η_{sp} is the quantum yield of spontaneous emission. The coefficient η' describes the escape of injected current carriers to emitters and depends on the laser structure design, doping, and temperature. The quantity of η_{sp} characterizes the relative role of useless recombination processes in

the active region, such as transitions through different defects and non-radiative AR. Increasing the temperature influences on the threshold value of the current carrier concentration that has, accordingly, an effect on η' and η_{sp} and on R_{sp} as well. In asymmetric QW heterostructures, the additional complex behavior appears due to electron-optical interaction of the QWs in the conditions of non-uniform excitation of the active region [2]. In this case, tunneling and carrier transport through modified barriers between the QWs provide specific changes in the threshold versus temperature [2, 4]. Below, conditions of uniform excitation of the varied width QWs are only examined.

Quantum-mechanical analysis of non-equilibrium electron processes in QWs of the lasers shows that at direct dipole optical transitions the threshold j_{th} changes practically directly proportional the operation temperature T where loses in the cavity are not very high. It can be used as a first step for the evaluation of the lower value of the lasing threshold.

The violation of conservation of the electron wave vector at optical transitions provides a second power dependence of $j_{th} \sim T^2$ [5]. Involving highlying excited subbands at the transitions increases power index of the dependence $j_{th}(T)$ and therefore functionally $j_{th} \sim T^n$, where n lies in the range of 1 to 3. The temperature decreasing of η' and η_{sp} has obviously a definite effect too. Additional behavior of the lasing threshold is introduced certainly by temperature changes in the cavity losses.

Often, the temperature dependence of the threshold is described by an exponential function with the characteristic parameter T_0. However, though it is a convenient empirical parameter, its value is ordinary indefinite, depends on the temperature operation interval, and widely varies for the same laser diode type. According to the determining of T_0 one has at a narrow temperature operation interval $T \approx T_{op}$ approximately $T_0 \approx T_{op}/n$.

To exclude the AR rate, we present the threshold in the form

$$j_{th} = \frac{e}{\eta'}\left(An_{th}^{n} + Cn_{th}^{3}\right), \qquad (2)$$

where n_{th} is the threshold sheet concentration of electrons. The coefficient A is determined by the optical transition probability and for direct dipole transitions ($n = 1$) it can be approximately taken as the Einstein coefficient A_{cv}, i. e., in this case, $A \approx A_{cv} \approx 1/\tau_{sp}$, where τ_{sp} is the threshold lifetime of current carriers at spontaneous radiative recombination [6]. In the limit case of no **k**-selection rule ($n = 2$), the coefficient A is also related to A_{cv} by a definite relation [5].

The last term in Eq. (2) describes the AR rate R since R is roughly proportional to n^3 [1]. As a rule, the AR coefficient C is determined in the activation approach, i. e., $C \approx C_0\exp(-E_{act}/kT)$ [1]. The activation energy is related to the energy of transitions between corresponding subband levels E_q through the formula $E_{act} \approx E_q\Delta m$, where Δm is the effective mass relation that is different for each of the AR processes. Generally, procedure of the determining of C in QW heterostructures, especially for strained laser systems, is rather complex and difficult [7].

If $n_{th} \sim T$, then we obtain

$$T_0 \approx \frac{T_{op}}{n + \left(1 - \eta_{sp}\right)\left(3 - n + E_{act}/kT_{op}\right)}. \qquad (3)$$

As seen, if the role of the AR becomes essential ($\eta_{sp} << 1$), the relation between the activation energy E_{act} and the thermal energy kT_{op} determines the value of the lasing threshold characteristic parameter T_0. On the other hand, from experimental results on the measurements of T_0 it is possible to evaluate the effective value of the activation energy of the AR processes.

2.2 Laser Structure

Numerical calculations have been performed for asymmetric bi-QW heterostructure lasers in the GaInAs–GaInAsP–InP system. The active region includes two QWs of widths d_1 =4 nm and d_2 = 9 nm and a barrier of the width d_b = 15 nm (Fig. 1).

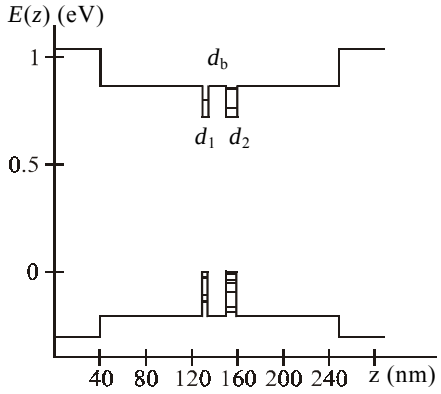

Fig. 1. Energy band diagram $E(z)$ in the active region of the $Ga_{0.47}In_{0.53}As$–$Ga_{0.18}In_{0.82}As_{0.4}P_{0.6}$–InP heterostructure laser. In different QWs of widths 4 and 9 nm, there are shown subband levels.

Energy levels in the QWs have been preliminarily determined in the effective mass approximation using standard parameters for semiconductor components [8] (Tabl. 1). In the QW of the 4-nm width, only one subband of electrons and light holes and two subbands of heavy holes are realized, in the QW of the 9-nm width the number of possible electron and light hole subbands is one more and the number of heavy hole subbands becomes up to four. The laser diodes operate at the wavelength near 1.55 μm and provide a widen tunable gain spectrum.

Table 1. Parameters for the calculations in the effective mass approximation, $T = 300$ K.

Energy gap E_g, eV			Band offset, eV	
QWs	barrier		ΔE_c	ΔE_v
0.718	1.060		0.137	0.205
Effective mass in units m_e				
electrons	heavy holes		light holes	
m_c	m_{vh}	m_{vht}	m_{vl}	m_{vlt}
0.043	0.307	0.051	0.040	0.116

More detailed energy band structure in the QWs was calculated according to the four-band **k·p** method [9, 10]. An example of the determined dispersion energy curves for the hole subbands in the 4-nm QW is shown in Fig. 2. The **k·p** calculation results are in good agreement with the evaluations of the subband energies in the effective mass approximation and were used for determining the gain and spontaneous radiative recombination spectra of the lasers.

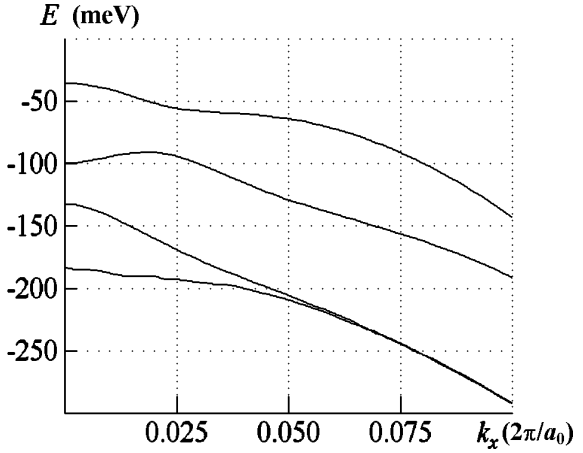

Fig. 2. Distribution of energy states $E(k_x)$ in the valence band for the QW of the width $d_1 = 4$ nm. $T = 300$ K. The wave vector component k_x is given in units $2\pi/a_0$, a_0 is the GaInAs crystal lattice period, $k_y = 0$.

2.3 Gain Spectrum

The gain coefficient at the light frequency ν and a definite TE- or TM-polarization in the QW of the width d_i ($i = 1, 2$) is given as follows [10, 11]

$$k(\nu) = \frac{e^2}{\varepsilon_0 c m_e^2 n_0 \nu d_i} \sum_{n,m} \int L(h\nu - E_{cv}) dE_{cv} \times$$
$$\times \int \left| \mathbf{M}_{nm} \right|^2 \left[f_e(E_{cn}(k_\parallel)) + f_h(E_{vm}(k_\parallel)) - 1 \right] \times \quad (4)$$
$$\times \frac{dk_\parallel}{(2\pi)^2} \delta\left(E_{cv} - E_{cn}(k_\parallel) + E_{vm}(k_\parallel) \right)$$

where n_0 is the refractive index of the active region, f_e and f_h are Fermi–Dirac functions for electrons and holes, $E_{cn}(k_\parallel)$ and $E_{vm}(k_\parallel)$ are energies of the states involved in the optical transitions, $|\mathbf{M}_{nm}|^2$ is the squared matrix element of the dipole transitions between electron and hole subbands with the quantum numbers n and m accordingly.

Here, the Lorentzian spectral broadening of the line emission is assumed and it is described by the function $L(h\nu - E_{cv})$, where E_{cv} is the energy of direct optical transitions between electron and hole subbands. The spectral broadening parameter Γ_{cv} is considered, as ordinary, to be of 10 meV [11]. Mention, that the squared matrix element of the transitions $|\mathbf{M}_{nm}|^2$ depends on the light polarization and reflects character of the involved hole states and effects of their mixing.

The spontaneous radiative recombination spectrum $r_{sp}(h\nu)$ is calculated similar to $k(\nu)$ with the exception of that the matrix element of the transitions is taken as for the isotropic radiation, i. e., $|\mathbf{M}_{nm}|^2$ in Eq. (4) is replaced by the value of the squared matrix element of the interband transitions $|\mathbf{M}_{cv}|^2 = m_e^2 E_g / 6 m_c$. Therefore, the spectral distribution of the spontaneous radiative recombination rate $r_{sp}(h\nu)$ in the QW of the width d_i is given in the form

$$r_{sp}(h\nu) = \frac{8\pi e^2 n_0 \nu}{\varepsilon_0 h m_e^2 c^3 d_i} \sum_{n,m} \int L(h\nu - E_{cv}) dE_{cv} \times$$
$$\times \int \left| \mathbf{M}_{cv} \right|^2 f_e(E_{cn}(k_\parallel)) f_h(E_{vm}(k_\parallel)) \times \quad (5)$$
$$\times \frac{dk_\parallel}{(2\pi)^2} \delta\left(E_{cv} - E_{cn}(k_\parallel) + E_{vm}(k_\parallel) \right)$$

The total spontaneous recombination rate R_{sp} is obtained by the summation of $r_{sp}(h\nu)$ over all possible energies of the emitted quanta $h\nu$.

The calculated spectra of the gain and spontaneous emission are shown in Fig. 3. In this case, the difference of the quasi-Fermi levels

which determines the excitation of the heterolaser active region equals $\Delta F = 0.96$ eV and corresponds to the conditions, where the total gain $g(\lambda_{st})$ at the lasing wavelength $\lambda_{st} = 1.47\mu m$ reaches the value of the cavity losses k_l up to 60 cm^{-1}.

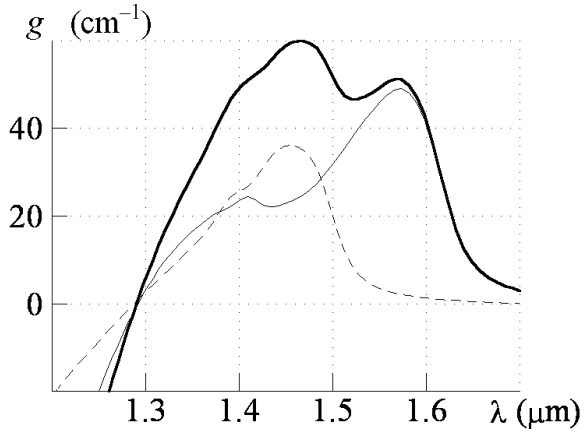

Fig. 3. Gain spectrum $g(\lambda)$ at the TE-mode at the excitation level $\Delta F = 0.96$ eV. $T = 300$ K, $k_l = 60$ cm^{-1}. Dashed curves correspond with $d_1 = 4$ nm, fine curves correspond with $d_2 = 9$ nm. $\Gamma_1 = 3.5\times10^{-3}$, $\Gamma_2 = 7.9\times10^{-3}$, sheet concentrations of electrons in the QWs are $n_1 = 1.23\times10^{13}$ cm^{-2} and $n_2 = 2.06\times10^{13}$ cm^{-2}, spontaneous recombination rates are $R_{sp1} = 0.75\times10^{22}$ s^{-1} cm^{-2} and $R_{sp2} = 1.89\times10^{22}$ s^{-1} cm^{-2}.

As seen, the wider QW gives a twice larger contribution in the total spontaneous recombination rate. As concerning the gain in the spectral region near the lasing wavelength, the contribution of the narrower QW is a half as much again as the contribution of the wider QW.

The waveguide gain at the threshold in a definite QW ($i = 1, 2$) is determined by both the gain coefficient $k(\lambda_{st})$ and the optical confinement factor Γ_i. The value of the optical confinement factor can be evaluated in the equivalent three-layer waveguide model. Using standard parameters for the described asymmetric QW heterostructure (Tabl. 1), we have for the TE-mode $\Gamma_1 = 3.5\times10^{-3}$ and $\Gamma_2 = 7.9\times10^{-3}$. Thought the optical localization of the electromagnetic wave is better in the 9-nm width QW, the value of $k(\lambda_{st})$ is more higher in the 4-nm width QW.

2.4 Auger Recombination Processes

Calculations of the AR rate in the laser active region have been made according to the conventional method [1]. The next interactions were considered, i. e., (CCCH) three electrons and one heavy hole, (CHHL) one electron, two heavy holes and one light hole, (CHHS) one electron, two heavy holes and one split-off-band hole, and (CLLS) one electron, two light holes and one split-off-band hole.

In the analytic representation, the coefficient C_0 for considered AR processes can be written approximately as [1]

$$C_0 = \frac{4e^4 \left|\mathbf{V}_\mathbf{T}\right|^2 \alpha}{\hbar k T \varepsilon^2}, \tag{6}$$

where ε is the dielectric constant of the crystal, $\mathbf{V}_T$ is the matrix element of the carrier interactions at the threshold energy for the definite AR process to take place The factor α for each processes CCCH, CHHL, CHHS, and CLLS is, accordingly, given

$$\begin{aligned}
&\alpha = \frac{(1+\mu_h)\mu_h}{(1+2\mu_h)^2}, \\
&\alpha = 2\left(\mu_l - 1 + \frac{2}{2+\mu_h}\right)\frac{\mu_h^2}{(2+\mu_h)\mu_l^2}, \\
&\alpha = 2\left(\mu_s - 1 + \frac{2}{2+\mu_h}\right)\frac{\mu_h^2}{(2+\mu_h)\mu_s^2}, \\
&\alpha = 2\left(\mu_s - 1 + \frac{2}{2+\mu_l}\right)\frac{\mu_l^2}{(2+\mu_l)\mu_s^2}, \\
&\mu_h = \frac{m_c}{m_{vht}}, \quad \mu_l = \frac{m_c}{m_{vlt}}, \quad \mu_s = \frac{m_c}{m_{vs}}.
\end{aligned} \tag{7}$$

Here, m_c is the effective mass of electrons, m_{vit} is the transverse component of the effective mass of heavy or light holes ($i = h$ or l), m_{vs} is the effective mass of holes in the split-off valence band.

The activation energy E_{act} of AR is related to the energy of transitions between corresponding subband levels E_q through the formula $E_{act} = E_q\delta_m$ and can be given in the following expressions for each processes CCCH, CHHL, CHHS, and CLLS, respectively,

$$\begin{aligned}
&E_{act} = E_h \frac{m_c}{m_c + m_{vht}}, \\
&E_{act} = E_l \frac{m_{vlt}}{m_c + 2m_{vht} - m_{vlt}}, \\
&E_{act} = (E_h - \Delta)\frac{m_{vs}}{m_c + 2m_{vht} - m_{vs}}, \\
&E_{act} = (E_l - \Delta)\frac{m_{vs}}{m_c + 2m_{vlt} - m_{vs}},
\end{aligned} \tag{8}$$

where E_h and E_l are the transition energies between electron and heavy and light hole states, Δ is the split-off separation energy. We assume at the calculations that above applied expressions in the Boltzmann approximation [1] can be also used for evaluations at the degenerate conditions in electron and hole subbands. Data of calculated parameters are presented in Tabl. 2.

Table 2: Activation parameters for different AR processes in the QWs, $T = 300$ K, $m_{vs} = 0.118m_e$, $\Delta = 0.361$ eV.

AR process type	δ_m	α
CCCH	0.458	0.215
CHHL	3.758	0.270
CHHS	4.089	0.256
CLLS	0.749	0.182
$d_1 = 4$ nm		
Energy E_q, eV	Activation energy E_{act}, eV	
0.838	0.384	
0.916	3.444	
0.477	1.951	
0.555	0.416	
$d_2 = 9$ nm		
Energy E_q, eV	Activation energy E_{act}, eV	
0.766	0.350	
0.803	3.018	
0.405	1.655	
0.442	0.331	

2.5 Auger Recombination Rate

Initially, evaluations of the AR rate R are carried out for each QW separately (Figs. 4 and 5), then the obtained results are included in the determining of the lasing threshold versus the temperature. Values of the current carrier concentration n/d were varied from 1×10^{19} to 7.5×10^{19} см$^{-3}$ (depending on the QW width) in the temperature range from 250 to 350 K, assuming the conditions of the electroneutrality in the laser active region.

For the asymmetric QW heterostructure under consideration, the temperature dependence of the AR rate occurs to be activation-like. The effective energy of activation E_{act} changes slightly with increasing the temperature and is affected by variations of E_q. Obviously, the energies E_q decrease at the temperature growth in parallel with the decreasing of E_g. The main contribution to the total AR rate is introduced by the CCCH and CLLS processes. Such a behavior is associated with the lower specific E_{act} that is caused with smaller values of δ_m as compared to other examined AR processes. For the QWs with widths of 4–9 nm and for considered intervals of non-equilibrium carrier concentrations n and temperatures T the effective energy of activation E_{act} lies in the range of 0.38 to 0.42 eV.

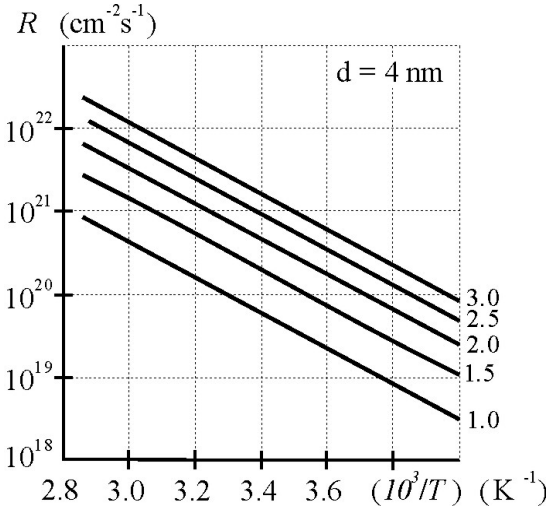

Fig. 4. Dependence of the total AR rate $R = Cn^3$ on the temperature T at different n (numbers in 10^{13} cm^{-2} at the curves), $d = 4$ nm.

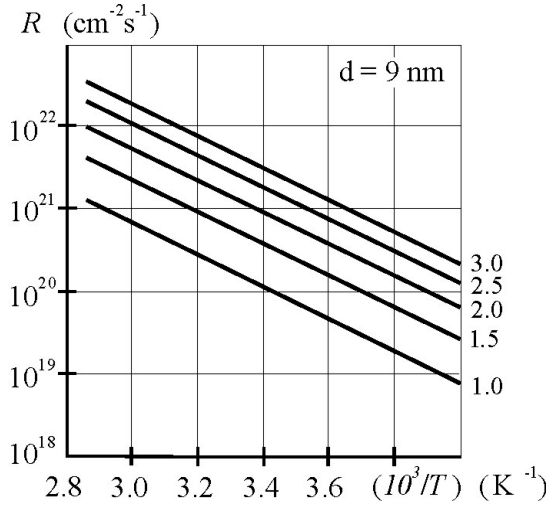

Fig. 5. Dependence of the total AR rate $R = Cn^3$ on the temperature T at different n (numbers in 10^{13} cm^{-2} at the curves), $d = 9$ nm.

The results connected with the dependence $R(d)$ show that in the range of the QW width d from 1 to 10 nm the AR rate increases since the levels structure changes. Firstly, the quantum-size level energy decreases. Secondly, it takes place the growth of the number of subbands in the QW and a new set of levels results in the total AR rate raising in turn. Therewith, however, an activation-like temperature dependence of the AR rate remains.

2.6 Temperature Dependencies

Numerical calculations show that with increasing the temperature of the laser diode active region the concentration of non-equilibrium current carriers in the QWs at the threshold increases approximately linearly with T (Fig. 6). The coefficient of the linearity depends on the width d and losses k_l. The threshold rate of the spontaneous radiative recombination in the QWs increases linearly with increasing the temperature as well. Accordingly, the lasing threshold current density j_{th} follows a similar law.

Mention, that the dependence $j_{th}(T)$ is markedly determined by the losses because of the power function $j_{th}(k_l)$. At the operation temperature $T = 300$ K and low losses $k_l = 40$ cm^{-1}, the lasing threshold is about of 1.8 kA/cm^2.

At larger losses k_l, the threshold $j_{th} = eR_{th}$ becomes rather high, e. g., at losses $k_l = 60$ cm^{-1}, the value j_{th} is equal to 4.2 kA/cm^2. At the higher operation temperatures and larger losses the lasing threshold grows up to 11 kA/cm^2. Therewith, the threshold concentration of non-equilibrium current carriers in the QWs markedly increases. As a result, contribution of the AR rate in the lasing threshold has to enhance the temperature dependence $j_{th}(T)$ (Fig. 7).

Comparison of the contribution of spontaneous radiative recombination and non-radiative AR processes in the lasing threshold indicates that the quantum yield of spontaneous emission η_{sp} maintains sufficiently high at the threshold until the operation temperature T_{op} does not exceed 360 K and the cavity loss k_l is lower than 80 cm^{-1}. In this case, we obtain that $\eta_{sp} > 0.4$. The suppressed role of the AR in the threshold results from the conditions that the basic contribution to the spontaneous radiative recombination provides by the wider QW but the gain is determined in general by the narrower QW. In that way, the important practical result is the conclusion on the possibility of decreasing the AR rate influence on the temperature dependence $j_{th}(T)$ in asymmetric multiple-QW heterostructure lasers having a high-quality cavity and operating at room temperatures.

With increasing the operation temperature and losses in the cavity the quantum yield of spontaneous emission η_{sp} markedly drops. Where $T_{op} = 360$ K and $k_l = 80$ cm^{-1}, the value of η_{sp} approaches 0.4. Then, taking into account $n = 1$ and $E_{act} \approx 0.4$ eV one can evaluate according to relation (3) the value $T_0 \approx 40$ K, i. e., the harmful decreasing of the characteristic temperature parameter of the threshold is revealed. It is clearly indicated in Fig. 7. Mention, that in the temperature interval where the AR contribution to the threshold is small ($T < 300$ K) the dependence $j_{th}(T)$ is weakening with the increase of k_l similar to bulk crystal injection lasers [12].

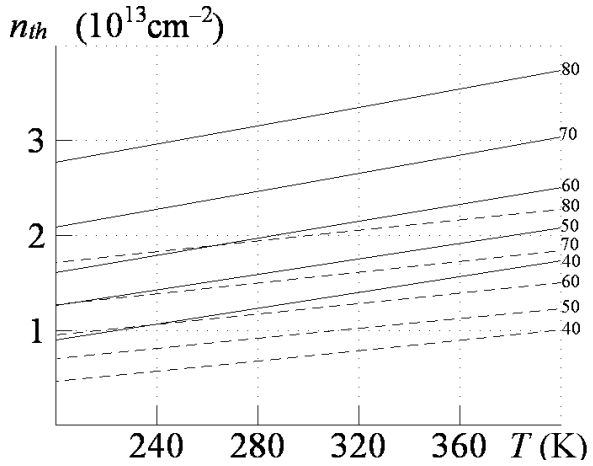

Fig. 6. Temperature dependencies of the threshold concentrations n_{th} in the QWs at different losses k_l (values on the curves in cm^{-1}). Dashed curves correspond with $d_1 = 4$ nm, solid curves correspond with $d_2 = 9$ nm. $\Gamma_1 = 3.5\times10^{-3}$, $\Gamma_2 = 7.9\times10^{-3}$.

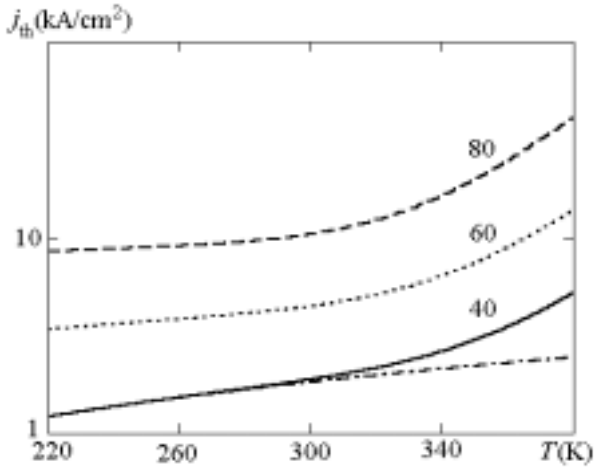

Fig. 7. Temperature dependence of the threshold current density $j_{th}(T)$ at different losses k_l (values at the curves in cm^{-1}). The lower dot-and-dash curve corresponds to $k_l = 40$ cm^{-1} and the absence of AR processes in the laser active region.

3 Conclusions

Asymmetric multiple-QW heterostructure lasers possess lower temperature sensitivity of the threshold and reduced role of the AR. The most important contribution of the AR rate to the threshold of the GaInAs-GaInAsP-InP heterolasers emitted at the wavelength near 1.55 μm is

attributed with the CCCH and CLLS processes. The AR rate increases practically as an activation-like function in the temperature interval 250 to 350 K and follows an exponential dependence on the QW width *d* varied from 4 to 9 nm.

As shown for the described asymmetric QW heterostructure lasers the influence of AR processes on the temperature behavior of the lasing threshold is not essential until the temperature of the active region is lower than 360 K and the cavity losses does not exceed 80 cm^{-1}.The presented analytical approach allows to evaluate the characteristic temperature of the lasing threshold and its relation with the effective activation energy of the AR processes.

References:

[1] G.P. Agrawal, N.K. Dutta, *Long-Wavelength Semiconductor Lasers*. John Wiley & Sons, N.-Y., 1986.

[2] V.K. Kononenko, A.A. Afonenko, I.S. Manak, S.V. Nalivko, Asymmetric multiple quantum well heterostructure laser systems: conception, performance, and characteristics, *Opto-Electron. Rev*., Vol.3, No.3, 2000, pp. 241–250.

[3] V.K. Kononenko, I.S. Manak, S.V. Nalivko, Design and characteristics of widely tunable quantum-well laser diodes, *Spectrochimica Acta, Part A: Mol. & Biomol. Spectroscopy*, Vol.55, No.10, 1999, pp. 2091–2096.

[4] S.V. Nalivko, A.A. Afonenko, I.S. Manak, Quantum-well lasers with low dependence of output power on temperature, *Tech. Phys. Lett.*, Vol.26, No.5, 2000, pp. 31–36.

[5] A.A. Afonenko, I.S. Manak, V.A. Shevtsov, V.K. Kononenko, Radiative recombination rate in quantum-well structures in the model without **k**-selection, *Semiconductors*, Vol.31, No.9, 1997, pp. 929–932.

[6] V.K. Kononenko, V.I. Tsvirko, Lifetime of current carriers at spontaneous radiative recombination in quantum wells, *Bull. RAS, Ser. Phys.*, Vol.67, No.2, 2003, pp. 223–226.

[7] A.D. Andreev, G.G. Zegrya, Auger recombination in strained quantum wells, *Semiconductors*, Vol.31, No.3, 1997, pp. 358–364.

[8] Z.-M. Li, T. Bradford, A comparative study of temperature sensitivity of InGaAsP and AlGaAs MQW lasers using numerical simulations, *IEEE J. Quantum Electron*., Vol.31, No.10, 1995, pp. 1841–1847.

[9] S.L. Chuang, Efficient band-structure calculations of strained quantum wells, *Phys. Rev. B,* Vol.43, No.12, 1991, pp. 9649–9661.

[10] S.V. Nalivko, I.S. Manak, A.L. Chizh, Influence of the band mixing effect on band structure and gain spectra of multiple-quantum-well heterostructures, *Lithuanian J. Phys.*, Vol.39, Nos.4–5, 1999, pp. 365–373.

[11] V.K. Kononenko, S.V. Nalivko, Spectral characteristics of asymmetric quantum-well heterostructure laser sources, *Proc. SPIE*, Vol.2693, 1996, pp. 760–767.

[12] V.P. Gribkovskii, V.K. Kononenko, Radiation lasing at the transitions through Gaussian impurity bands, *J. Appl. Spectrosc.*, Vol.12, 1970, pp. 45–56.